nip, a Symbiotic *Medicago truncatula* Mutant That Forms Root Nodules with Aberrant Infection Threads and Plant Defense-Like Response[1]

Harita Veereshlingam, Janine G. Haynes, R. Varma Penmetsa, Douglas R. Cook, D. Janine Sherrier, and Rebecca Dickstein*

Department of Biological Sciences, University of North Texas, Denton, Texas 76203–5220 (H.V., R.D.); Delaware Biotechnology Institute, University of Delaware, Newark, Delaware 19711 (J.G.H., D.J.S); and Department of Plant Pathology, University of California, Davis, California 95616 (R.V.P., D.R.C.)

To investigate the legume-Rhizobium symbiosis, we isolated and studied a novel symbiotic mutant of the model legume *Medicago truncatula*, designated *nip* (numerous infections and polyphenolics). When grown on nitrogen-free media in the presence of the compatible bacterium *Sinorhizobium meliloti*, the *nip* mutant showed nitrogen deficiency symptoms. The mutant failed to form pink nitrogen-fixing nodules that occur in the wild-type symbiosis, but instead developed small bump-like nodules on its roots that were blocked at an early stage of development. Examination of the *nip* nodules by light microscopy after staining with X-Gal for *S. meliloti* expressing a constitutive GUS gene, by confocal microscopy following staining with SYTO-13, and by electron microscopy revealed that *nip* initiated symbiotic interactions and formed nodule primordia and infection threads. The infection threads in *nip* proliferated abnormally and very rarely deposited rhizobia into plant host cells; rhizobia failed to differentiate further in these cases. *nip* nodules contained autofluorescent cells and accumulated a brown pigment. Histochemical staining of *nip* nodules revealed this pigment to be polyphenolic accumulation. RNA blot analyses demonstrated that *nip* nodules expressed only a subset of genes associated with nodule organogenesis, as well as elevated expression of a host defense-associated phenylalanine ammonia lyase gene. *nip* plants were observed to have abnormal lateral roots. *nip* plant root growth and nodulation responded normally to ethylene inhibitors and precursors. Allelism tests showed that *nip* complements 14 other *M. truncatula* nodulation mutants but not *latd*, a mutant with a more severe nodulation phenotype as well as primary and lateral root defects. Thus, the *nip* mutant defines a new locus, *NIP*, required for appropriate infection thread development during invasion of the nascent nodule by rhizobia, normal lateral root elongation, and normal regulation of host defense-like responses during symbiotic interactions.

The symbiosis that develops between leguminous plants and soil rhizobia to form a nitrogen-fixing root nodule is a complex and unique interaction. The interaction begins with an exchange of signals between rhizobia and plants in the rhizosphere. Flavonoid compounds released by the host plant stimulate the expression of *nod* genes in an appropriate rhizobial species, resulting in the production of bacterial Nod factors. Nod factors, lipochitooligosaccharide molecules, are able to induce specific responses in the host plant, including root hair deformation and cortical cell division. Infection conduits called infection threads originate in deformed root hairs that curl to form a so-called shepherd's crook and facilitate entry of rhizobia into the root. Infection thread initiation and growth require living rhizobia that are synthesizing specific Nod factors (Ardourel et al., 1994; Limpens et al., 2003). Most infection threads abort in root epidermal cells, with only a small fraction of the infections proceeding to the interior of the root (Vasse et al., 1993; Penmetsa and Cook, 1997). For the infection threads that penetrate the interior of the root, the course by which they proceed is predetermined by cytoplasmic bridges or preinfection threads; these allow infection threads to pass through outer cortical cells toward the inside of the root (Kijne, 1992; van Brussel et al., 1992). When infection threads reach cells in the newly formed nodule primordium, they become confined to the intercellular space between cells (Kijne, 1992). As an infection thread ceases growth, irregular structures including unwalled droplets of infection thread matrix material containing rhizobia are formed. These are engulfed by the plant host plasma membrane, forming symbiosomes in a process resembling endocytosis. The peribacteroid membrane surrounding the symbiosome is initially formed by the plasma membrane of the host cell and expands by fusion with newly synthesized vesicles carrying peribacteroid membrane nodule-specific proteins (Brewin, 1998). Within symbiosomes, the rhizobia differentiate into

[1] This work was supported by University of North Texas Faculty Research Funds (to R.D.), the University of Delaware Research Foundation, and a National Institutes of Health BRIN (no. RR16472–02) to the Delaware Biotechnology Institute (to D.J.S).

* Corresponding author; e-mail beccad@unt.edu; fax 940–565–3821.

Article, publication date, and citation information can be found at www.plantphysiol.org/cgi/doi/10.1104/pp.104.049064.

bacteroids that are capable of fixing nitrogen. Reviews on legume root nodule development and the rhizobial infection process are available (Brewin, 1991; Hirsch, 1992; Kijne, 1992; Brewin, 1998; Gage and Margolin, 2000; Gage, 2004).

The means by which invading rhizobia are able to avoid triggering most of the legume root's host defense mechanisms are not understood. In a normal legume-rhizobia interaction, there are some detectable plant defense responses. Very localized hypersensitive-like reactions accompany aborted infections in epidermal cells and may be part of the plant host's autoregulation of nodule number (Vasse et al., 1993). When mutant rhizobia deficient in surface molecules, specifically exopolysaccharide (EPS) or lipopolysaccharide (LPS), interact with plant hosts, a larger and more generalized plant defense response is often activated (Niehaus et al., 1993; Perotto et al., 1994). The role of surface polysaccharides in the *Rhizobium*-legume symbiosis has recently been reviewed (Fraysse et al., 2003).

Genes and processes involved in lateral root formation may also be involved in nodule formation. Like nodule development, lateral root development is influenced by hormones as well as the nutritional status of the plant. Unlike nodules that develop from cortical cell divisions, lateral roots usually develop from divisions in the pericycle. Both types of divisions take place opposite a protoxylem pole, but lateral roots have a central arrangement of vascular bundles, whereas nodules have peripheral vascular bundles (Hirsch, 1992; Casimiro et al., 2003). When lateral roots emerge, tissues in the lateral root primordium become distinct, and the root cap, root meristem, and central stele are established.

In 1990, *Medicago truncatula* was proposed as a model legume, particularly for studying the *Rhizobium*-legume symbiosis, because of its small genome size (approximately 500 Mbp, $n = 8$), self-compatibility, relatively short generation time, ability to be transformed, and the well-characterized nature of its microsymbiont, *Sinorhizobium meliloti* (Barker et al., 1990). Since then, many genetic and genomic tools have been developed for *M. truncatula* (Cook, 1999); recently, detailed genetic maps have been produced (Thoquet et al., 2002; Choi et al., 2004), a genetically anchored physical map is emerging, and the euchromatic regions of *M. truncatula*'s genome are being sequenced. *M. truncatula* produces the indeterminate type of nodule with a persistent meristem and, therefore, all stages of nodule development can be studied within a single mature nodule.

Here, we describe the isolation of a novel *M. truncatula* mutant, *nip*, and present data on its phenotype. *nip* plants respond to *S. meliloti* by producing abnormal nodules in which numerous aberrant infection threads are produced, with very rare rhizobial release into host plant cells. It has an abnormal defense-like response in root nodules as well as defects in lateral root development.

RESULTS

Isolation of the Recessive *nip* Mutant

Ethyl methane sulfonate-generated *M. truncatula* plants from the A17 genetic background were screened for nodulation phenotypes in the M_2 generation by inoculating them with an *S. meliloti* strain containing the constitutive *hemA*::*lacZ* construct (Boivin et al., 1990; Penmetsa and Cook, 1997, 2000). Putative mutants that had white nodule bumps instead of pink leghemoglobin-containing nitrogen-fixing nodules were screened at 10 d postinoculation (dpi) by staining roots with X-Gal for the presence of *Sinorhizobium*. Plants without rhizobia in their nodules and plants with lower than wild-type amounts of rhizobia were propagated and rescreened in the M_3 and M_4 generations for their nodulation phenotypes. *nip* was originally characterized from the C bulk as mutant C90, having small nodules/bumps on its roots with limited nodule invasion by rhizobia, short primary roots, and defective lateral roots. It was found to be proficient in the mycorrhizal symbiosis (M. Harrison, personal communication). Based on the phenotype (see below), the gene responsible for the mutant phenotype in C90 was named *nip*, for numerous infections and polyphenolics, in accordance with nomenclature rules for *M. truncatula* (VandenBosch and Frugoli, 2001), and registered with the *M. truncatula* gene nomenclature index (http://www.genome.clemson.edu/affiliated_cugi/medicago).

nip was back-crossed twice (BC_2), utilizing the male-sterile *tap* mutation in the wild-type A17 background (Penmetsa and Cook, 2000) to ensure true crossing. *nip*, in the A17 *M. truncatula* genetic background, was also crossed into A20, a different polymorphic ecotype of *M. truncatula*, in order to facilitate future genetic-mapping studies. The A17/A20 pair forms the basis of one of the genetic maps of *M. truncatula* (Choi et al., 2004). Wild-type:*nip* segregated approximately 3:1 in F_2 populations obtained in each back-cross to genotype A17 and in crosses to ecotype A20, consistent with a single-gene recessive mutation (Table I). Back-crossed *nip* plants were more robust in terms of overall growth than the original mutant. Characterization of the *nip* phenotype was carried out on plants BC_2, except where noted.

Representative wild-type and *nip* BC_2 plants grown in an aeroponic chamber were photographed at 15 dpi (Fig. 1, A and B). *nip* roots showed variation in root length from plant to plant and were observed to have abnormal lateral roots. Unlike wild-type plants that had clearly emerged lateral roots (Fig. 1C), most *nip* plants had either no lateral roots, although lateral root primordia were visible (Fig. 1D), or had shorter lateral roots (Fig. 1B) than wild type (Fig. 1A). Instead of effective, pink, leghemoglobin-containing nodules as were found in wild type (Fig. 1E), *nip* developed straw-colored root nodules/bumps containing a brown pigment (Fig. 1F), suggesting an accumulation

Table I. *Segregation of nip phenotype in nip × wild-type crosses*

χ^2 calculated for 3:1 ratio wild-type nodule:mutant nodule; $P > 0.05$ when $\chi^2 < 3.84$.

Cross, Progeny Tested	Wild-Type Nodules	Mutant Nodules	χ^2
nip × *Mtap*, (BC_1) F_2	80	24	0.21
nip × *Mtap*, (BC_2) F_2	70	21	0.16
nip × A20, F_2	54	14	0.02

of polyphenolic compounds. Cosegregation of the lateral root defect with the nodulation defect was found in all *nip* F_2 progeny tested in all crosses.

nip Nodules Accumulate Polyphenolic Compounds and Have Large, Proliferating Infection Threads That Rarely Release Rhizobia

When grown without nitrate and in the presence of compatible rhizobia, *nip* plants exhibited reduced vigor with chlorotic leaves that are characteristic of nitrogen deficiency. These symptoms were alleviated by supplementation with nitrate fertilizer and are indicative of a defect in the ability to form an effective nitrogen-fixing symbiosis. Growth of *nip* plants in the presence of nitrate fertilizer had no effect on the lateral root phenotype (data not shown).

To evaluate *nip*'s nodulation phenotype, *nip* plants were grown in an aeroponic system and inoculated with *S. meliloti* carrying the *hemA*::*lacZ* fusion. Staining with X-Gal at 15 dpi revealed a proliferation of *S. meliloti* inside numerous infection threads in the nodule primordia (Fig. 2, A and B). The *nip* nodule primordia emerged from the root only after prolonged nodule development times, at or after 25 dpi. In contrast, emerged elongated wild-type A17 nodules were filled with the blue-staining *S. meliloti* at 15 dpi.

In order to more closely examine the extent of infection, *nip* and wild-type nodules were stained with nucleic acid-binding dye SYTO-13 and examined by laser-scanning confocal microscopy (LSCM). Stained rhizobia fluoresced in the green spectrum using this technique, while polyphenolics and cell walls fluoresced in the red spectrum, pseudocolored blue in the figure to enhance detail (Fig. 3). By 13 dpi, fully mature wild-type nodules had emerged from the surface of the primary root and infected cells were characterized by high rhizobial cellular occupancy (Fig. 3A). In contrast, despite an examination of over 160 *nip* nodules, we failed to find clear examples of infected host cells in the *nip* mutant. As was seen using the *hemA*::*lacZ* marker and X-Gal staining, infection thread numbers were found to be substantially higher in *nip* (Fig. 3B), and LSCM revealed abnormal infection thread morphology in *nip* nodules. Infection threads, including the original infection thread that originates in the root epidermis, were thickened relative to wild-type threads with abnormal bulbous protrusions (Fig. 3C) that became more pronounced over time with an increase in diameter of the threads and the size of the protrusions (Fig. 3D). *nip* nodules were found to emerge from the root epidermis only late in development, and were also found to have large areas of

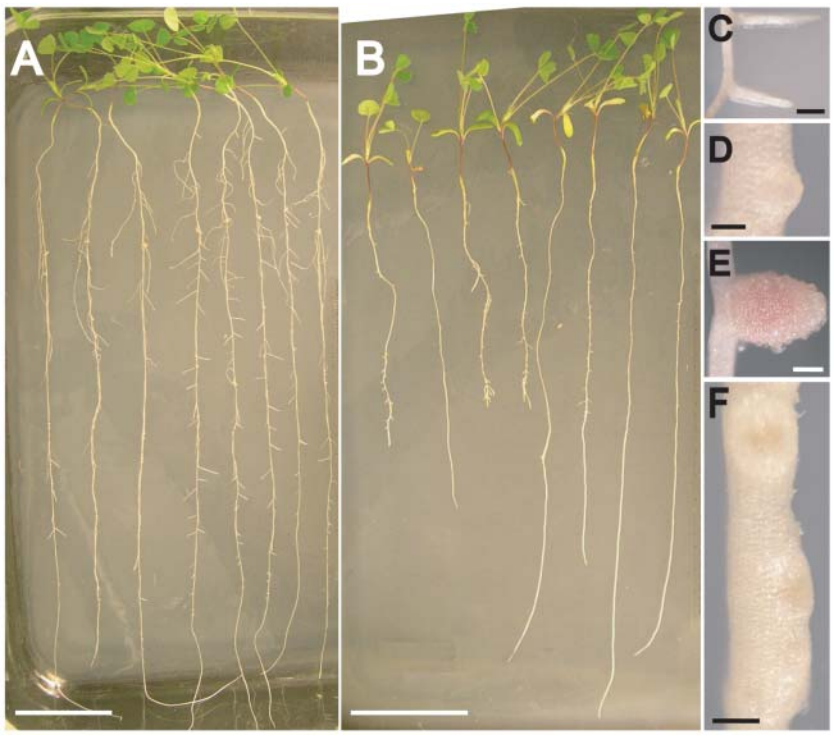

Figure 1. Phenotype of *nip* and wild-type (A17) plants 15 dpi with *S. meliloti*. Plants were grown in aeroponic chambers as described in "Materials and Methods" and placed on an agar support for photography. A, Wild-type plants. Bar = 5.0 cm. B, *nip* plants. Bar = 5.0 cm. C, Wild-type primary root with emergent lateral roots. Bar = 1.0 mm. D, *nip* lateral root primordium. Bar = 0.25 mm. E, Wild-type nodule. Bar = 0.50 mm. F, *nip* nodules/bumps. Note the presence of a dark pigment at the distal ends of the nodules. Bar = 0.50 mm.

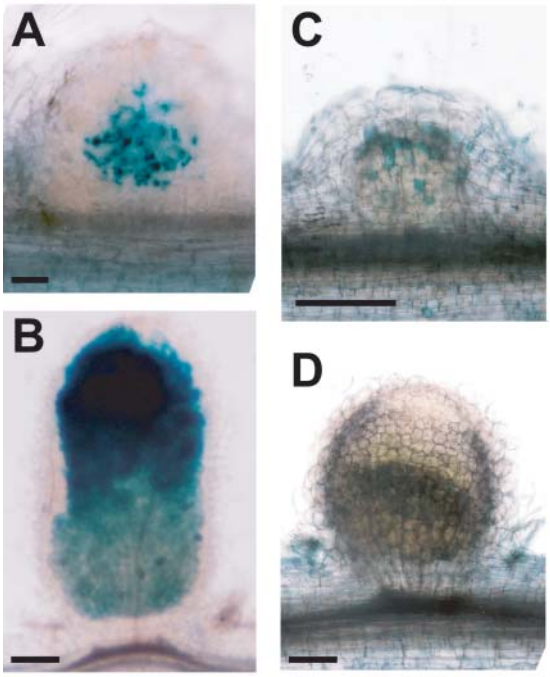

Figure 2. Rhizobial infection (A and B) and polyphenolic accumulation (C and D) in *nip* and wild-type nodules. *nip* and A17 wild-type plants inoculated with *S. meliloti* carrying the *hemA*::*lacZ* reporter were hand-sectioned and stained with X-Gal at 15 dpi. *S. meliloti* stain blue. A, *nip* nodule; B, A17 nodule. *nip* and A17 wild-type plants were inoculated with *S. meliloti*, fixed, and stained with potassium permanganate followed by methylene blue. Polyphenolics stain blue in this procedure. C, *nip* nodule; D, A17 nodule. Bars = 0.2 mm.

autofluorescing cells, suggesting an induction of the plant defense response. The autofluorescing cells were localized near cells with infection threads, but did not themselves contain threads.

To determine if the autofluorescence and the accumulation of brown pigment represented an accumulation of polyphenolic compounds, nodules were stained with potassium permanganate using a method that results in blue precipitates at sites of polyphenols (Fig. 2, C and D). Individual cells in the nodule cortex of *nip* nodules stained heavily for polyphenolics, with other cell types displaying no staining (Fig. 2C). In contrast, in wild-type A17 nodules, no polyphenolic staining was detected in any of the cells in the nodule (Fig. 2D).

To further explore the *nip* nodule phenotype and examine the interface between the infection threads and plant host cells in detail, studies using transmission electron microscopy (TEM) on 15 and 21 dpi *nip* nodules were carried out. No differences between the 15 and 21 dpi nodules were observed and data from 15 dpi nodules are presented here. Wild-type nodules developed normally, and by 15 dpi had produced fully mature nodules exhibiting the typical developmental zones: meristem, prefixation zone (Fig. 4A), interzone, and nitrogen-fixation zone (Fig. 4, B and I). In contrast, *nip* nodules commonly remained unemerged at this stage and exhibited no distinct developmental zones; rather, the nodule interior most closely resembled an enlarged prefixation zone (Fig. 4, C and E). Infection droplets in the wild-type nodule were confined to a narrow zone below the meristem, were generally small, and exhibited normal release of bacteria (Fig. 4A), whereas droplets in *nip* were seen throughout the nodule interior and were often enlarged with excess matrix material (Fig. 4C). Wild-type infection threads were generally narrow and grew in a linear pattern through cells (Fig. 4B). In contrast, *nip* infection threads were much more numerous, often unusually wide and irregularly shaped (Fig. 4D), and commonly grew in a serpentine pattern (Fig. 4E). At high magnification, wild-type infection droplets (Fig. 4F) were similar in appearance to *nip* infection droplets, but *nip* infection droplets rarely released bacteria into host cells. In one instance, limited release of bacteria was seen in one cell of a *nip* nodule (Fig. 4H), but the bacteria were small and undifferentiated when compared to the mature fixation zone of a wild-type nodule (Fig. 4I). At this stage, *nip* plants were severely nitrogen stressed and it is unlikely that this limited infection could have progressed to a normally infected cell. In addition to abnormal threads, *nip* nodules also exhibited abnormal membrane profiles within vacuoles in the uninfected nodule periphery, several cell layers removed from the threads. Membrane profiles were seen in the vacuoles and were suggestive of cell death in these regions (Fig. 4, J and K). These cells correspond to the region in Figure 3 that contained autofluorescent compounds and to the region in Figure 2 that stained for polyphenolics.

nip Plants Have Normal Shoots and Abnormal Lateral Roots

Growth characteristics were investigated by growing F_3 plants derived from the BC_2 generation and from crosses into ecotype A20, using the aeroponic system with nitrate-free media in the presence of rhizobia. The results are shown in Tables II and III. In plants propagated from BC_2, *nip* primary shoots were found to be approximately the same size as wild type at 5 and 10 dpi, and averaged 75% of wild type at 15 dpi, presumably reflecting a nitrogen deficiency (Table II).

As was noted above (see Fig. 1), in F_3 plants derived from the BC_2 population, *nip* plants showed root abnormalities. To further investigate the *nip* root phenotype, *nip* plants with the most normal-looking root systems were crossed to ecotype A20. Several F_2 plants resulting from this cross were observed that had primary roots of similar length to wild type and possessed lateral roots. To determine the correlation between altered lateral root development with symbiotic phenotype, 47 individual F_3 progeny from these F_2 plants were examined for their root phenotypes (Table III). The F_3 progeny had roots that averaged a similar

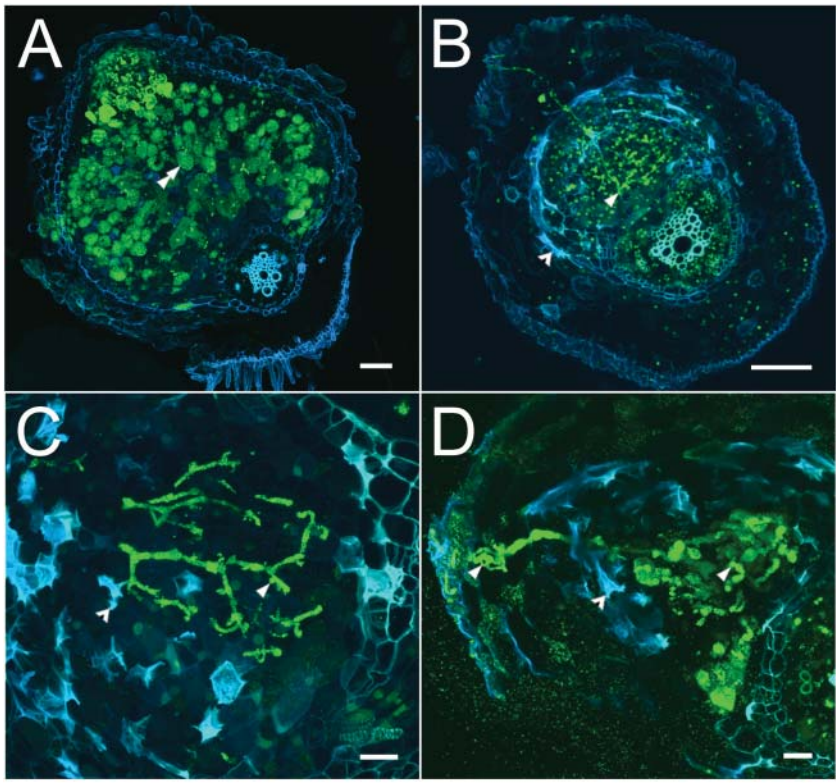

Figure 3. Confocal light micrographs of *M. truncatula* wild-type (A17) and mutant (*nip*) nodules. A, Wild-type nodule 13 dpi. Nodule has emerged from the root and shows normal mature infected cells containing intracellular bacteroids (green). A typical infected cell is indicated by the double arrowhead. Bar = 100 μm. B, *nip* nodule 13 dpi demonstrating abnormal nodule formation. The nodule is infected with bacteria and there are an unusually high number of threads present (single arrowhead). Mutant nodules often did not emerge from the root and autofluorescence (blue) is observed in cells around the infection threads (barbed arrowhead). Bar = 100 μm. C, Higher magnification of *nip* mutant nodule 13 dpi showing abundant threads that terminate without release of bacteria into plant cell cytoplasm. Threads are thickened, exhibit abnormal bulges (arrowhead), and are flanked by cells exhibiting autofluorescence (blue). Bar = 20 μm. D, High magnification view of *nip* mutant nodule 29 dpi showing highly enlarged and distorted threads. Single arrowhead indicates an infection thread; barbed arrowhead indicates blue autofluorescence in nodule cells. Bar = 20 μm.

length as wild type, 18.4 ± 4.4 cm, compared to 19.7 ± 1.7 cm for A17, and 18.6 ± 3.5 cm for A20. However, only 11, or approximately 25% of the 47 individual F_3 plants, had lateral roots, although, as before, lateral root primordia were evident. When present, the lateral roots occurred at a lower frequency than wild type (Table III) and were shorter in length compared to wild type (data not shown). This strongly suggests that the lateral root defect in *nip* is incompletely penetrant.

Ethylene Responsiveness Is Similar in *nip* and Wild Type

Previous studies have shown that the plant hormone ethylene plays a central role in regulation of successful infections as well as root growth in *M. truncatula* (Penmetsa and Cook, 1997, 2000; Oldroyd et al., 2001; Penmetsa et al., 2003). To determine if the *nip* mutant was altered in ethylene responses, *nip* root length and nodule number were measured in the presence of various concentrations of the ethylene inhibitor L-α-(2-aminoethoxyvinyl)-Gly (AVG) and in the presence of the ethylene precursor 1-aminocyclopropane carboxylic acid (ACC). The results, shown in Figure 5, demonstrate a similar percentage increase in root length and nodule number in *nip* BC_2 plants as compared to wild type (A17) in the presence of increasing AVG concentration. When *nip* plants were grown in the presence of ACC, a similar decrease in root length and nodule number in *nip* plants, as compared to wild-type A17, was observed (data not shown). Together, the AVG and ACC data suggest that the *nip* mutant phenotype is unlikely to be mediated by altered ethylene biosynthesis or perception.

nip Nodule Gene Expression Studies Indicate a Block to Nodule Differentiation and Elevated Levels of a Transcript Associated with Plant Defense

To evaluate the progression of *nip* nodule development at the transcriptional level, the expression of four genes associated with nodule development and two genes associated with plant host defense were investigated in *nip* and wild-type nodulating roots. The *ENOD40* gene is correlated with formation of nodule and lateral root primordia (Crespi et al., 1994; Fang and Hirsch, 1998). The *MtN12* gene encodes a nodule-specific extensin associated with the IT matrix (Gamas et al., 1996; Rathbun et al., 2002). The *ENOD2* gene is expressed in the nodule parenchyma (van de Wiel et al., 1990) and is a marker for early stages of nodule organogenesis. *ENOD8* is expressed in infected nodule cells in *M. truncatula* relatively early in nodule development (Dickstein et al., 1993, 2002) and is a marker for infected cell formation (L. Coque, K. Wilson, and R. Dickstein, unpublished data). As shown in Figure 6, *ENOD40* and *MtN12* are expressed at comparable levels in *nip* and wild-type nodulating roots, while expression of *ENOD2* and *ENOD8* are not detectable in *nip* nodulating roots. These data are consistent with *nip* roots responding to rhizobial signals by producing nodule primordia that become invaded by rhizobia in infection threads. The absence of *ENOD2* and *ENOD8*

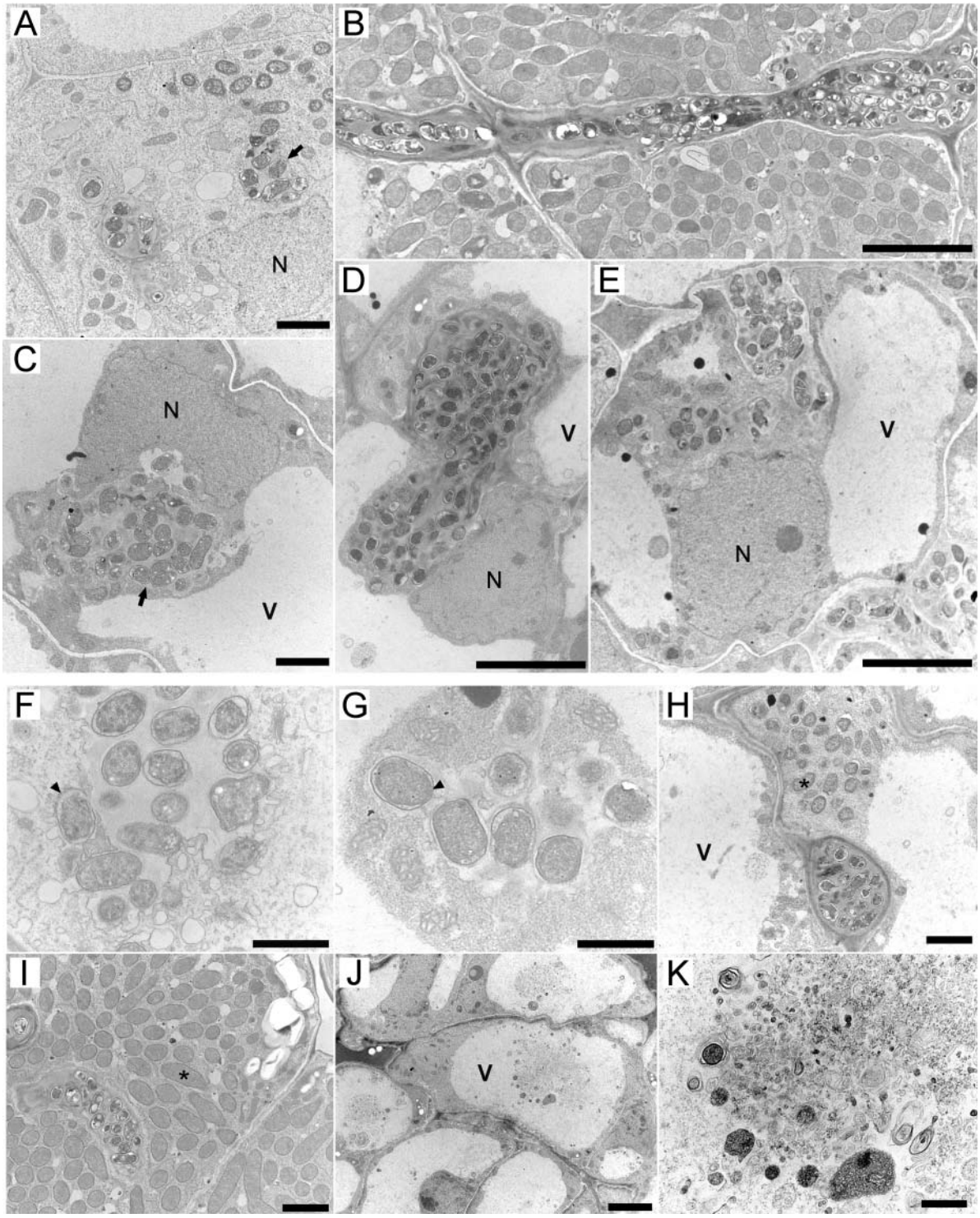

Figure 4. TEMs of ultrathin nodule sections from 15 dpi. A, Invasion zone of a wild-type nodule. Arrow indicates an infection droplet releasing bacteria into the plant cell cytoplasm. N, Nucleus. Bar = 2 μm. B, Remnant infection thread in the fixation zone of a wild-type nodule. Note that the thread is straight and relatively narrow. Bar = 5 μm. C, Cells of the extensive invasion zone in *nip* nodules. Arrow indicates an enlarged infection droplet-like structure in a *nip* nodule cell. V, Vacuole. Bar = 5 μm. D, Enlarged and irregular infection thread in *nip* nodule. Bar = 5 μm. E, Meandering infection thread in *nip* nodule. Bar = 5 μm. F, Wild-type infection droplet. Arrow indicates bacterium being released. Bar = 1 μm. G, Infection droplet-like structure in *nip* nodule. Arrow indicates a comparable bacterium to that shown in F. Bar = 1 μm. H, Rare instance of limited bacterial release in a *nip* nodule. *, Released bacterium. Bar = 2 μm. I, Large, mature bacteroids in fixation zone of wild-type nodule. *, Bacteroid. Bar = 2 μm. J, Cells at the *nip* nodule periphery with membrane profiles in the vacuoles. Bar = 5 μm. K, Higher magnification image of the vacuolar membrane profiles in *nip* cells. Bar = 1 μm.

Table II. *Shoot growth characteristics of nip plants compared to wild type*

Plants were grown in aeroponic chambers as described in "Materials and Methods." Four or five plants were harvested and measured for each time point. Averages ± SDs are given.

dpi	A17 Shoot Length	*nip* Shoot Length
	cm	*cm*
5	2.0 ± 0.4	2.1 ± 0.4
10	5.2 ± 0.4	5.0 ± 0.8
15	6.4 ± 1.1	4.7 ± 1.0

expression, each of which is associated with specific aspects of nodule organogenesis, is consistent with *nip* nodules being halted at a very early stage of nodule differentiation.

Cytological evaluation demonstrated an unusual plant defense-like response in *nip* nodules (Figs. 2C, 3, and 4, J and K). Therefore, expression of two genes associated with plant host defense was studied in nodulating *nip* and wild-type roots. Elevated levels of pathogenesis-related protein-10 (*PR-10*) and Phe ammonia lyase (*PAL*) are both associated with plant host defense and plant stress (Hammond-Kosack and Jones, 2000). *PR-10* mRNA accumulation in *nip* nodulating roots was found to be comparable to wild-type nodulating roots. In contrast, *PAL* expression was found to increase dramatically during *nip* nodule development compared to wild type. Because *PAL* encodes the enzyme catalyzing the first step in phenylpropanoid metabolism, the elevated levels of *PAL* mRNA are consistent with the accumulation of polyphenolics detected in *nip* nodules.

Allelism Tests

Although *nip* has a different phenotype from other legume mutants studied by several groups in the Medicago scientific community, it is possible that it is allelic to another mutant. To test this possibility, *nip* was crossed to other mutants and two to six independent F_1 progeny from each cross were scored for nodulation phenotype. Of particular interest were mutants that are able to initiate nodulation but are defective in rhizobial invasion or later steps in the symbiosis. Genetic crosses of the *nip* mutant to each of several *M. truncatula* mutants, *lin*, *rit*, *bit*, TE7 (*Mtsym1*), *dnf1*, *dnf2*, *dnf3*, *dnf4*, *dnf5*, *dnf6*, or *dnf7* (Benaben, 1994, 1995; Mitra and Long, 2004; Kuppusamy et al., 2004), were carried out. All F_1 progeny from each cross were found to have wild-type nodulation, indicating that *nip* was not allelic to any of these loci. Additionally, *nip* complemented *dmi1*, *dmi2*, and *nsp1*, which are defective in Nod factor signal transduction (Catoira et al., 2000). Notably, *nip* did not complement *latd*. *latd* is a *M. truncatula* mutant with phenotypes somewhat similar to, but much more severe than, *nip*. (J. Harris, personal communication and unpublished observations).

DISCUSSION

We identified a novel symbiotic mutant in *M. truncatula* called *nip*. The monogenic and recessive *nip* mutant is able to initiate nodule development, but is not competent to attain functional nitrogen-fixing nodules when grown in the presence of the compatible *Rhizobium* sp., *S. meliloti*. As our studies using light, confocal and electron microscopy show, the *nip* mutant is capable of developing nodule primordia and initiating rhizobial invasion through plant-derived infection threads. However, *nip* infection threads are thicker than wild type and characterized by abnormal bulbous protrusions and unusual branching. The block to nodule development is most likely at release of rhizobia from infection threads and endocytosis into the host cytoplasm. The *nip* mutant is very slightly leaky, rarely allowing release of rhizobia into host cells, but neither the rhizobia nor the host cells appeared to differentiate in response to release. Our data do not allow us to distinguish whether the infection thread characteristics observed are a consequence of

Table III. *Root system characteristics of individual nip × A20 F_2 nip nodule phenotype plants' F_3 progeny*

All *nip* plants measured were progeny of *nip* × A20 F_2 plants having lateral roots and wild-type length primary roots. Plants were grown in aeroponic chambers as described in "Materials and Methods." The *nip* and control plants' characteristics were measured at 10 dpi.

Plant(s)	Number Plants Examined	Number of Plants with Lateral Roots	Number of Lateral Roots per Plant (When Present)	Root Lengths
				cm
A17	9	9	4.7 ± 3.6	19.7 ± 1.7
A20	10	10	3.3 ± 1.5	18.6 ± 3.5
nip × A20, *nip* no. 1	7	2	1, 3	16.7 ± 1.5
nip × A20, *nip* no. 2	14	5	1, 1, 2, 3, 3	22.3 ± 3.8
nip × A20, *nip* no. 3	6	2	2, 7	20.9 ± 4.0
nip × A20, *nip* no. 4	13	2	1, 1	15.7 ± 4.1
nip × A20, *nip* no. 5	7	0		16.3 ± 2.9

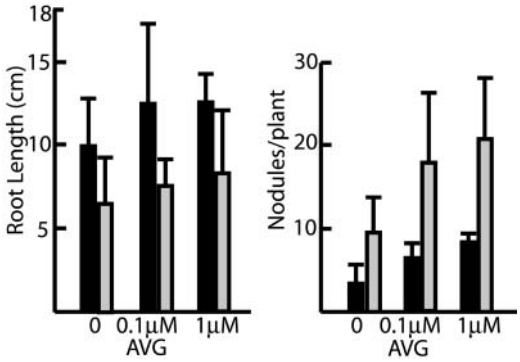

Figure 5. Root length and nodule number in plants grown in the presence of AVG. Wild-type A17 (black bars) and *nip* plants (gray bars) were grown on solid media in petri dishes containing the indicated concentrations of AVG with their roots shielded from light. Four or five plants were measured for each concentration of AVG tested.

the failure to release rhizobia from the threads or if infection thread characteristics, including size, proliferation, or biochemical constitution, cause the rhizobia not to be released.

nip nodules show evidence of an abnormal plant host defense-like response. We noted that the cells with the defense-like response, those that stain for polyphenolics, are autofluorescent and with a vacuolar accumulation of membrane fragments, are only a subset of cells within the nodule and are generally adjacent to cells not undergoing a defense-like response. This feature of defense-like response in *nip* resembles the hypersensitive response, where cells undergoing programmed cell death are interspersed among living cells (Hammond-Kosack and Jones, 2000). The cells with features of defense response were found several cell layers from the abnormal infection threads. Moreover, the *nip*-specific induction of *PAL*, a transcript frequently associated with host responses to pathogens, provided additional circumstantial evidence of a host defense response. It is unclear whether the defense-like response is a primary effect of the *nip* mutation or is a secondary response to the block to nodule development or to the abnormal infection threads.

Ethylene is a plant hormone that has been implicated in regulation of plant defense, rhizobial infections, and root growth (Penmetsa and Cook, 1997; Oldroyd et al., 2001; Penmetsa et al., 2003). Growth of *nip* plants on media containing ethylene inhibitors or precursors revealed similar effects as on wild-type plants. Thus, it is unlikely that ethylene metabolism or perception is compromised in the *nip* mutant.

nip plants showed an approximate 2-fold increase in nodule number as compared to wild-type plants (e.g. see Fig. 5). Similar increases in nodule number have been noted in studies with other legume and rhizobial mutants that form ineffective nodules (Dickstein et al., 1988; Benaben et al., 1995; Kuppusamy et al., 2004). Similar to other symbiotic mutants, the lack of mature nodule meristems in *nip* may lead to recurrent nodule initiation, a downstream effect of the absence of nitrogen-fixing nodules, rather than a specific effect of the *nip* mutation.

Nodule-specific marker genes for nodule primodia (*ENOD40*) and infection thread formation (*MtN12*) were expressed in nodulating *nip* root systems. Genes that are associated with nodule organogenesis (*ENOD2, ENOD8*) were not. Lack of *ENOD2* expression in *nip* nodules is consistent with recent studies that showed nodule-like structures formed in *M. truncatula* in response to *S. meliloti exo* mutants are associated with an absence of *ENOD2* expression (Mitra and Long, 2004). The studies presented here demonstrate that, in *M. truncatula*, formation of nodule primordia invaded by rhizobia within infection threads is not sufficient for *ENOD2* or *ENOD8* expression.

The *nip* nodule phenotype is similar in some respects to defective nodules elicited by other mutations in either the bacterial or legume symbiotic partners. Both *S. meliloti* EPS I-deficient mutants and LPS-deficient *R. leguminosarum* mutants induce nodule structures on alfalfa and pea, respectively, showing signs of a host defense reaction. Thickened infection thread-like structures containing rhizobia were observed in intercellular spaces in the nodule structures, with some rhizobia able to form symbiosomes, although at a higher frequency than was observed in the *nip* mutant (Niehaus et al., 1993; Perotto et al., 1994). *S. meliloti* LPS mutants form Fix^- nodules on *M. truncatula* with enlarged infection threads that released rhizobia, but failed to form symbiosomes properly, and with a host defense reaction (Niehaus et al., 1998). Given the similarity of the *nip* nodules to nodules elicited by EPSI- or LPS-deficient *Rhizobium* sp., it is tempting to speculate that the defect in *nip* is in a receptor or part of a signal transduction pathway for molecules on the surface of the *Rhizobium* sp. However, alternative explanations remain a possibility because auxotrophic rhizobial mutants, like the *S. meliloti hemA* mutant controlling

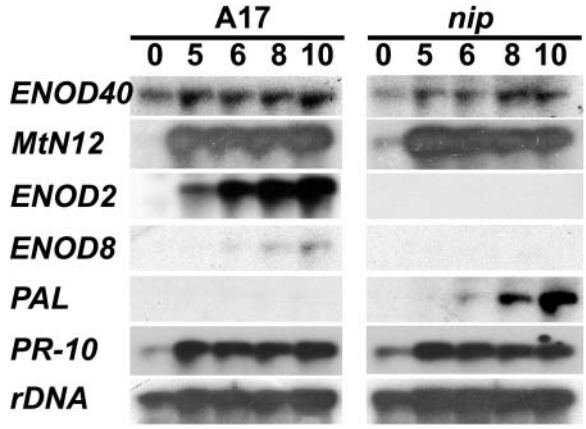

Figure 6. RNA-blot analysis of gene expression during *nip* nodule development. Gel blots were prepared from 20 μg of total RNA extracted from A17 or *nip* roots inoculated with *S. meliloti* at the indicated times after inoculation (dpi). Blots were hybridized sequentially with radiolabeled *ENOD40, MtN12, ENOD2, ENOD8, PAL*, and *PR-10* probes, with rDNA serving as the loading control.

the first step of heme biosynthesis (Dickstein et al., 1991), as well as a rhizobial mutant defective in the synthesis of signal peptides (Muller et al., 1995), also produce nodules containing infection threads without rhizobial endocytosis into host plant cells.

The *nip* nodule phenotype is also similar to that of other *M. truncatula* symbiotic mutants, especially the *lin* and *Mtsym1* (TE7) mutants. *lin* forms nodule primordia in which infection thread development halts at the root epidermis, apparently before the blockage in *nip*. Similar to *nip*, nodulating *lin* root systems express genes associated with nodule primordium formation but not the *ENOD2* and *ENOD8* genes associated with nodule differentiation (Kuppusamy et al., 2004). By contrast, nodule development in *Mtsym1* appears to progress further than *nip* as *Mtsym1* nodules are invaded by rhizobia that senesce upon release (Benaben et al., 1995). Interestingly, *Mtsym1* nodules exhibit evidence of defense-like responses, including deposition of polyphenolic substances, similar to the current observation of polyphenolic accumulation in *nip* nodules. Benaben (1994) observed *ENOD2*, but not *ENOD8*, expression in certain *MtSym1* nodules, while a more recent study of *Mtsym1* nodules concluded that *ENOD2* was not expressed (Mitra and Long, 2004). The difference between the two studies may be the result from different growth conditions. Based on developmental phenotypes, we propose that the *NIP* gene acts after *LIN* and before *MtSYM1*. The *M. truncatula dnf* mutants have all been found to express *ENOD2* (Mitra and Long, 2004); thus, *NIP* acts before the *DNF* genes.

Because of the diverse effects of the *nip* mutation on infection thread morphology, nodule differentiation, marker gene expression, polyphenolic accumulation, and lateral root growth, we speculate that *NIP* may have a regulatory role in root and nodule development. *NIP* is also required to suppress a defense-like response. It is unclear whether *NIP* is a direct suppressor of the defense-like response or whether the infection thread proliferation and failure to release rhizobia resulting from *NIP* loss of function triggers the response. The molecular identification of *NIP* should further elucidate the intersection between symbiotic nodule and lateral root development and may yield insight into aspects of the balance between symbiosis and host defense.

MATERIALS AND METHODS

Plant Material and Growth Conditions

Medicago truncatula A17 wild-type plants were germinated and grown in aeroponic growth chambers misted with an inorganic nutrient media lacking NH_4NO_3 (Lullien et al., 1987) as described previously (Dickstein et al., 2002; Catalano et al., 2004). Briefly, seeds greater than 3 months old were scarified with concentrated H_2SO_4 for 8 min, rinsed in sterile water, surface sterilized with 6% sodium hypochlorite for 1 min, and rinsed with sterile water. *nip* plants were treated similarly, but the sodium hypochlorite treatment was omitted. Seeds were imbibed with sterile water with gentle rotation for 5 to 7 h at ambient temperature, then stored in water at 4°C for 16 to 24 h, plated on petri dishes, and then left in the dark at room temperature for 14 to 15 h for germination. Freshly harvested seeds (1–2 weeks after pod maturation) were left in sterile deionized water for 24 h on a rotating shaker and then germinated in the dark at room temperature for 14 to 15 h. For vernalization, plants were maintained in a moist chamber for 2 weeks at 4°C. Plants were placed into aeroponic chambers when their roots were at least 0.5 cm long and misted with a nitrogen-free nutrient solution (Lullien et al., 1987). Plants were maintained in a growth room at 22°C on a 16-h-light and 8-h-dark schedule under Phillips Agro-Lite bulbs (Phillips, Somerset, NJ) at 60 μmol m^{-2} s^{-1}. For nodulation studies, plants were inoculated with *Sinorhizobium meliloti* strain ABS7 (Bekki et al., 1987), strain Rm2011 (Rosenberg et al., 1981), or *S. meliloti*/pXLDG4 (Boivin et al., 1990; Penmetsa and Cook, 1997) 5 d after germination. Infected roots and nodules were harvested at the indicated times after inoculation. Plants used for confocal microscopy and TEM studies were grown as above with some modifications. A17 seeds were scarified for 6 min and surface sterilized for 3 min with 6% sodium hypochlorite and rinsed thoroughly with sterile water after each step. Both *nip* and wild-type A17 seeds were imbibed in sterile water at ambient temperature for 5 h, stored at 4°C overnight, and rinsed with sterile water over a 6-h period prior to spreading on a petri dish. Seeds were sown immediately after germination on aeroponic chambers with Lullien solution containing NH_4NO_3, changed to Lullien solution without NH_4NO_3 after 5 d, and inoculated 9 d postsowing with *S. meliloti* Rm2011.

For the ethylene inhibitor and precursor studies, plant growth and nodulation studies were performed on agar plates. The same media were used with the appropriate AVG or ACC concentrations and solidified with 1% w/v phytagar (Invitrogen, Carlsbad, CA). The root portion was shaded by covering the bottom half of plates with aluminum foil. Growth conditions were the same as for aeroponic growth.

Histochemical Staining

S. meliloti/pXLDG4 containing the *hemA*::*lacZ* reporter was visualized on plant roots as described (Boivin et al., 1990). Briefly, whole roots were vacuum infiltrated for three cycles of 30 s with 2.5% glutaraldehyde in 0.1 M PIPES (pH 7.2), fixed for 1 h, and rinsed in 0.1 M PIPES (pH 7.2) twice. Samples were then incubated in staining solution containing 50 mM potassium ferricyanide, 50 mM potassium ferrocyanide, 0.08% X-Gal, and 0.1 M PIPES (pH 7.2) for 16 h at room temperature. Samples were rinsed in 0.1 M PIPES (pH 7.2), cleared with 2.4% sodium hypochloride for 5 min, sectioned on a vibratome (model 1000; Vibratome, St. Louis), sectioned by hand or left whole, mounted on glass slides with coverslips, and observed under an Olympus BX50 microscope (Olympus, Melville, NY) using bright field.

For LSCM studies, nodulated roots were prepared and imaged as described (Haynes et al., 2004). Briefly, nodulated roots were harvested into 80 mM PIPES (pH 7.0) and nodules were hand-sectioned longitudinally. Nodule halves were stained with 1 μL mL^{-1} SYTO-13 (Molecular Probes, Eugene, OR) in PIPES buffer for 15 m, transferred to a Lab-Tech chambered no. 1.5 coverglass system (Nalge/Nunc, Naperville, IL), and imaged on an inverted Zeiss LSM 510 NLO laser-scanning microscope (Carl Zeiss, Jena, Germany).

Detection of polyphenolics was accomplished by staining with potassium permanganate to visualize polyphenols as described (Vasse et al., 1993). Briefly, whole roots were fixed in 2.5% glutaraldehyde, 0.01 M PIPES (pH 7.2), and stained in 0.04% potassium permanganate for 1 h, rinsed in 0.01 M PIPES (pH 7.2), then stained with 0.01% aqueous solution of methylene blue. The roots were cleared with 2.4% sodium hypochlorite for 3 min and visualized as above.

TEM

Nodules were produced aeroponically as described and harvested at 5, 10, 15, and 21 dpi. Nodulated roots were harvested into a solution of 4% formaldehyde and 1% glutaraldehyde in 80 mM PIPES (pH 7.0). Wild-type nodules were dissected from the root system and cut longitudinally to aid in infiltration. *nip* nodules were generally unemerged and formed in clusters, so nodulated portions of the root were cut into small segments for fixation. Nodules were vacuum infiltrated in fixative 4 × 2 min and fixed overnight at 4°C with rotation. Nodules were rinsed 3 × 15 min with distilled water, stained 4 h with 1% OsO_4 (aq), rinsed 3 × 15 min with distilled water, dehydrated in a graded series of acetone, and infiltrated with a graded series of Epon Araldite resin (Mollenhauer, 1964). Samples were polymerized in Epon Araldite resin for 48 h at 60°C. Nodules were sectioned with glass knives and then 70-nm sections were collected using a Diatome diamond knife (Diatome-U.S., Fort Washington, PA) on a Reichert Ultracut E ultramicrotome. Sections were

collected onto hexagonal gold grids and were counterstained with alkaline lead citrate (Reynolds, 1963) for 7 min and 0.5% uranyl acetate (aq) for 12 min. Samples were visualized and documented on a Zeiss CEM 902 TEM.

RNA Extraction and Blots

RNA was extracted and northern blots prepared with 20 μg RNA for each sample as previously described (Dickstein et al., 2002). DNA was labeled for hybridization by random priming (Feinberg and Vogelstein, 1983). The probes used were *ENOD40* (Crespi et al., 1994); *ENOD2*, GenBank accession number X12580 (Dickstein et al., 1988); *ENOD8*, GenBank accession number AF064775 (Liu et al., 1998); *MtN12* (Gamas et al. 1996); *PAL* (GenBank accession no. BF635112); *PR-10* (GenBank accession no. AW587229), with rDNA (Dickstein et al., 1991) as loading control.

Genetic Analysis

Mutants were crossed into the male sterile *M. truncatula* A17 mutant (*MtAp*) as previously described (Penmetsa and Cook, 2000). Male-sterile, nodule-deficient F_2 mutants that resulted from this cross were used as female parents in crosses with A17 and other mutants. Plants were evaluated for phenotype 10 dpi by examining their roots for the presence of white bumps or pink nitrogen-fixing nodules by eye or with the aid of a dissecting microscope.

ACKNOWLEDGMENTS

We gratefully acknowledge Kate VandenBosch, in whose lab some mutant screening was performed; Colby Starker, Giles Oldroyd, Sharon Long, Kate VandenBosch, Thierry Huguet, and Jeanne Harris for seed of various *M. truncatula* nodulation and nitrogen-fixation mutants; Jannon Fuchs and Harry Schwark for help with the vibratome; Kate VandenBosch, Joe Clouse, and Pascal Gamas for cDNA clones; Jeanne Harris for insightful discussions; and Kirk Czymmek and Carol Carlson for assistance with confocal microscopy.

Received July 8, 2004; returned for revision August 12, 2004; accepted August 23, 2004.

LITERATURE CITED

Ardourel M, Demont N, Debelle F, Maillet F, de Billy F, Prome JC, Denarie J, Truchet G (1994) *Rhizobium meliloti* lipooligosaccharide nodulation factors: different structural requirements for bacterial entry into target root hair cells and induction of plant symbiotic developmental responses. Plant Cell **6:** 1357–1374

Barker DG, Bianchi S, London F, Dattee Y, Duc G, Essad S, Flament P, Gallusci P, Genier G, Muel X, Tourneur J, Denarie J, et al (1990) *Medicago truncatula*, a model plant for studying the molecular genetics of the *Rhizobium*-legume symbiosis. Plant Mol Biol Rep **8:** 40–49

Bekki A, Trinchant J-C, Rigaud J (1987) Nitrogen fixation (C_2H_2 reduction) by *Medicago* nodules and bacteroids under sodium chloride stress. Physiol Plant **71:** 61–67

Benaben V (1994) Caracterisation cytologique et moleculaire du mutant symbiotique TE7 de *Medicago truncatula*. PhD thesis. Universite Paul Sabatier, Toulouse, France

Benaben V, Duc G, Lefebvre V, Huguet T (1995) TE7, an inefficient symbiotic mutant of *Medicago truncatula* Gaertn. cv Jemalong. Plant Physiol **107:** 53–62

Boivin C, Camut S, Malpica CA, Truchet G, Rosenberg C (1990) *Rhizobium meliloti* genes encoding catabolism of trigonelline are induced under symbiotic conditions. Plant Cell **2:** 1157–1170

Brewin NJ (1991) Development of the legume root nodule. Annu Rev Cell Biol **7:** 191–226

Brewin NJ (1998) Tissue and cell invasion by *Rhizobium*: the structure and development of infection threads and symbiosomes. *In* HP Spaink, A Kondorosi, PJJ Hooykaas, eds, The *Rhizobiaceae*, Molecular Biology of Model Plant-Associated Bacteria. Kluwer Academic Publishers, Dordrecht, The Netherlands, pp 417–429

Casimiro I, Beeckman T, Graham N, Bhalerao R, Zhang H, Casero P, Sandberg G, Bennett MJ (2003) Dissecting *Arabidopsis* lateral root development. Trends Plant Sci **8:** 165–171

Catalano C, Lane WS, Sherrier DJ (2004) Biochemical characterization of symbiosome membrane proteins from *Medicago truncatula* root nodules. Electrophoresis **25:** 519–531

Catoira R, Galera C, de Billy F, Penmetsa RV, Journet EP, Maillet F, Rosenberg C, Cook D, Gough C, Denarie J (2000) Four genes of *Medicago truncatula* controlling components of a Nod factor transduction pathway. Plant Cell **12:** 1647–1666

Choi H-K, Kim D, Uhm T, Limpens E, Lim H, Kalo P, Penmetsa VR, Seres A, Kulikova O, Bisseling T, Kiss G, Cook DR (2004) A sequence-based genetic map of *Medicago truncatula* and comparison of marker colinearity with *Medicago sativa*. Genetics **166:** 1463–1502

Cook DR (1999) *Medicago truncatula*—a model in the making! Curr Opin Plant Biol **2:** 301–304

Crespi MD, Jurkevitch E, Poiret M, d'Aubenton-Carafa Y, Petrovics G, Kondorosi E, Kondorosi A (1994) *enod40*, a gene expressed during nodule organogenesis, codes for a non-translatable RNA involved in plant growth. EMBO J **13:** 5099–5112

Dickstein R, Bisseling T, Reinhold VN, Ausubel FM (1988) Expression of nodule-specific genes in alfalfa root nodules blocked at an early stage of development. Genes Dev **2:** 677–687

Dickstein R, Hu X, Yang J, Ba L, Coque L, Kim D-J, Cook DR, Yeung AT (2002) Differential expression of tandemly duplicated Enod8 gene in *Medicago*. Plant Sci **163:** 333–343

Dickstein R, Prusty R, Peng T, Ngo W, Smith ME (1993) ENOD8, a novel early nodule-specific gene, is expressed in empty alfalfa nodules. Mol Plant Microbe Interact **6:** 715–721

Dickstein R, Scheirer DC, Fowle WH, Ausubel FM (1991) Nodules elicited by *Rhizobium meliloti* heme mutants are arrested at an early stage of development. Mol Gen Genet **230:** 423–432

Fang Y, Hirsch AM (1998) Studying early nodulin gene ENOD40 expression and induction by Nodulation factor and cytokinin in transgenic alfalfa. Plant Physiol **116:** 53–68

Feinberg AP, Vogelstein B (1983) A technique for radiolabeling DNA restriction endonuclease fragments to high specific activity. Anal Biochem **132:** 6–13

Fraysse N, Couderc F, Poinsot V (2003) Surface polysaccharide involvement in establishing the rhizobium-legume symbiosis. Eur J Biochem **270:** 1365–1380

Gage DJ (2004) Infection and invasion of roots by symbiotic, nitrogen-fixing rhizobia during nodulation of temperate legumes. Microbiol Mol Biol Rev **68:** 280–300

Gage DJ, Margolin W (2000) Hanging by a thread: invasion of legume plants by rhizobia. Curr Opin Microbiol **3:** 613–617

Gamas P, de Carvalho-Niebel F, Lescure N, Cullimore J (1996) Use of a subtractive hybridization approach to identify new *Medicago truncatula* genes induced during root nodule development. Mol Plant Microbe Interact **9:** 223–242

Hammond-Kosack K, Jones JDG (2000) Responses to plant pathogens. *In* BB Buchanan, W Gruissem, RL Jones, eds, Biochemistry and Molecular Biology of Plants. American Society of Plant Biologists, Rockville, MD, pp 1102–1165

Haynes JG, Cyzmmek KJ, Carlson CA, Veereshlingam H, Dickstein R, Sherrier DJ (2004) A novel method for rapid analysis of legume root nodule development using confocal microscopy. New Phytol **163:** 661–668

Hirsch AM (1992) Developmental biology of legume nodulation. New Phytol **122:** 211–237

Kijne JW (1992) The *Rhizobium* infection process. *In* G Stacey, HJ Evans, RH Burris, eds, Biological Nitrogen Fixation. Chapman and Hall, London, pp 349–398

Kuppusamy KT, Endre G, Prabhu R, Penmetsa RV, Veereshlingam H, Cook DR, Dickstein R, VandenBosch KA (2004) *LIN*, a *Medicago truncatula* gene required for nodule differentiation and persistence of rhizobial infections. Plant Physiol **136:** 3682–3691

Limpens E, Franken C, Smit P, Willemse J, Bisseling T, Geurts R (2003) LysM domain receptor kinases regulating rhizobial Nod factor-induced infection. Science **302:** 630–633

Liu C, Yeung AT, Dickstein R (1998) The cDNA sequence of *Medicago truncatula* cv. *Jemalong* Enod8, a gene associated with nitrogen fixing root nodule organogenesis. Plant Physiol **117:** 1127

Lullien V, Barker DG, de Lajudie P, Huguet T (1987) Plant gene expression in effective and ineffective root nodules of alfalfa (*Medicago sativa*). Plant Mol Biol **9:** 469–478

Mitra RM, Long SR (2004) Plant and bacterial symbiotic mutants define three transcriptionally distinct stages in the development of the *Medicago truncatula*/*Sinorhizobium meliloti* symbiosis. Plant Physiol **134:** 595–604

Mollenhauer H (1964) Plastic embedding mixtures for use in electron microscopy. Stain Technol **39:** 111–114

Muller P, Klaucke A, Wegel E (1995) Tn*phoA*-induced symbiotic mutants of *Bradyrhizobium japonicum* that impair cell and tissue differentiation in *Glycine max* nodules. Planta **197:** 163–175

Niehaus K, Kapp D, Puhler A (1993) Plant defence and delayed infection of alfalfa pseudonodules induced by an exopolysaccharide (EPSI)-deficient *Rhizobium meliloti* mutant. Planta **190:** 415–425

Niehaus K, Lagares A, Puhler A (1998) A *Sinorhizobium meliloti* lipopolysaccharide mutant induces effective nodules on the host plant *Medicago sativa* (alfalfa) but fails to establish a symbiosis with *Medicago truncatula.* Mol Plant Microbe Interact **11:** 906–914

Oldroyd GED, Engstrom EM, Long SR (2001) Ethylene inhibits the Nod factor signal transduction pathway of Medicago truncatula. Plant Cell **13:** 1835–1849

Penmetsa RV, Cook DR (1997) A legume ethylene-insensitive mutant hyperinfected by its rhizobial symbiont. Science **275:** 527–530

Penmetsa RV, Cook DR (2000) Production and characterization of diverse developmental mutants of *Medicago truncatula.* Plant Physiol **123:** 1387–1398

Penmetsa RV, Frugoli JA, Smith LS, Long SR, Cook DR (2003) Dual genetic pathways controlling nodule number in *Medicago truncatula.* Plant Physiol **131:** 998–1008

Perotto S, Brewin NJ, Kannenberg EL (1994) Cytological evidence for a host defense response that reduces cell and tissue invasion in pea nodules by lipopolysaccharide-defective mutants of *Rhizobium leguminosarum* strain 3841. Mol Plant Microbe Interact **7:** 99–112

Rathbun E, Naldrett MJ, Brewin NJ (2002) Identification of a family of extensin-like glycoproteins in the lumen of *Rhizobium*-induced infection threads in pea root nodules. Mol Plant Microbe Interact **15:** 350–359

Reynolds ES (1963) The use of lead citrate at high pH as an electon opaque stain in electron microscopy. J Cell Biol **17:** 208–212

Rosenberg C, Boistard P, Denarie J, Casse-Delbart F (1981) Genes controlling early and late functions in symbiosis are located on a megaplasmid in *Rhizobium meliloti.* Mol Gen Genet **184:** 326–333

Thoquet P, Gherardi M, Journet E-P, Kereszt A, Ane J-M, Prosperi J-M, Huguet T (2002) The molecular genetic linkage map of the model legume *Medicago truncatula*: an essential tool for comparative legume genomics and the isolation of agronomically important genes. BMC Plant Biol **2:** 1

van Brussel AAN, Bakhuizen R, van Spronsen PC, Spaink HP, Tak T, Lugtenberg BJJ, Kijne JW (1992) Induction of pre-infection thread structures in the leguminous host plant by mitogenic lipo-oligosaccharides of *Rhizobium.* Science **257:** 70–72

van de Wiel C, Norris JH, Bochenek B, Dickstein R, Bisseling T, Hirsch AM (1990) Nodulin gene expression and ENOD2 localization in effective, nitrogen-fixing and ineffective, bacteria-free nodules of alfalfa. Plant Cell **2:** 1009–1017

VandenBosch KA, Frugoli J (2001) Standards and guidelines for genetic nomenclature for the model legume *Medicago truncatula.* Mol Plant Microbe Interact **14:** 1364–1367

Vasse J, Billy F, Truchet G (1993) Abortion of infection during the *Rhizobium meliloti*-alfalfa symbiotic interaction is accompanied by a hypersensitive reaction. Plant J **4:** 555–566